Approximate Formulas for the Far Field and Gain of Open-Ended Rectangular Waveguide

ARTHUR D. YAGHJIAN, MEMBER, IEEE

Abstract—**Approximate formulas are derived for the far field and gain of standard, open-ended, rectangular waveguide probes operating within their recommended usable bandwidth. (Such probes are commonly used in making near-field antenna measurements.) The derivation assumes first-order azimuthal dependence for the fields, and an *E*-plan pattern given by the traditional Stratton–Chu integration of the transverse electric (TE_{10}) mode. The *H*-plane pattern is estimated by two different methods. The first method uses a purely *E*-field integration across the end of the waveguide. The second, more accurate method approximates the fringe currents at the shorter edges of the guide by isotropically radiating line sources. The amplitude of the line sources is determined by equating the total power radiated into free space to the net input power to the waveguide. Comparisons with measurements indicate that for *X*-band and larger waveguide probes, both methods predict on-axis gain to about 0.2 dB accuracy. The second method predicts far-field power patterns to about 2 dB accuracy in the region 90° off boresight and with rapidly increasing accuracy toward boresight.**

I. INTRODUCTION

MOST NEAR-FIELD antenna measurements are made using open-ended, unflanged, rectangular waveguide probes. They are simple, rugged, and inexpensive to produce (or reproduce), they have a broad far-field power pattern with no nulls in the forward hemisphere over their recommended usable bandwidth, they scatter relatively little radiation back to the test antenna being measured, and they have a respectable gain of about 6–8 dB. However, unlike far-field measurements where only the on-axis gain of the probe is required, near-field measurements require, in general, the complex far field in the forward hemisphere of the probe in order to compensate for its response in the near field. Specifically, for each microwave frequency at which the test antenna is to be measured, the appropriate standard rectangular waveguide probe is chosen and its far-field pattern, gain, and reflection coefficient are measured as a necessary part of the complete near-field measurement procedure.

The reflection coefficient of the transverse electric (TE_{10}) mode can be measured accurately and rapidly over the waveguide bandwidth using, e.g., an automatic network analyzer, but the measurement of probe pattern and gain is a rather tedious, time-consuming operation, especially when the fields of the test antenna are desired at several frequencies for which the probe has not been previously calibrated.

To alleviate this chore of measuring the probe far fields, at least when extremely high accuracy is not required, we have derived reasonably accurate formulas for the far-field pattern gain of open-ended, standard rectangular waveguides over their recommended usable bandwidths. Comparison with measured data indicates that the formulas approximate the far field of *X*-band (WR-90) and larger standard waveguide with a 0.2 dB accuracy in on-axis gain. This accuracy represents a significant improvement over the 2 to 3 dB accuracy of previous approximate formulas derived entirely by aperture integration with the Stratton–Chu formulas [1, sec. 8.14; 2], or by a parallel-plate edge diffraction technique [3]. For *Ku*-band (WR-62) and smaller standard waveguides, the approximate formulas derived in this paper may become less accurate because the wall thickness of these smaller waveguides becomes a large enough fraction of their height to appreciably affect the edge currents [4].

Manuscript received May 17, 1983; revised December 19, 1983.

The author is with the Electromagnetic Sciences Division, Rome Air Force Development Center, Hanscom AFB, MA 01731.

II. DERIVATION OF FAR-FIELD FORMULAS

The geometry of the open-ended rectangular waveguide is shown in Fig. 1. The inner dimensions of the waveguide are given by width a and height b. The perfectly conducting waveguide walls are assumed to have a negligible thickness compared to the smaller dimension b. The origin of the xyz rectangular coordinate system is chosen at the center of the open end of the waveguide, and the spherical coordinates of the position vector $\bar{r}$ to any point in space is denoted by (r, θ, ϕ). The waveguide operates at a frequency f that lies within the recommended usable bandwidth of the TE_{10} mode with the electric field in the y direction.

We take a semi-empirical approach to approximate the far fields and absolute gain of the open-ended waveguide.[1] Consider the far field of the waveguide expressed as a sum of spherical multipoles located at the origin. Because the transverse dimensions of the waveguide are less than a wavelength, only the multipoles of lower order azimuthal (ϕ) dependence will contribute significantly to the far field. Moreover, because all but the first-order ($\sin\phi - \cos\phi$ dependent) multipoles have a null in the on-axis (z) direction, one would expect significant coupling to free space only from these first-order multipoles. Under this assumption and the symmetry of the rectangular waveguide excited by the TE_{10} mode, the far fields of the open-ended waveguide can be expressed approximately in the following simple form [1, sec. 7.11]:

$$\bar{E}(\bar{r}\to\infty) = \frac{e^{ikr}}{kr}\left[E_E(\theta)\sin\phi\hat{e}_\theta + E_H(\theta)\cos\phi\hat{e}_\phi\right] \tag{1a}$$

$$\bar{H}(\bar{r}\to\infty) = \frac{e^{ikr}}{kr}\frac{1}{Z_0}\left[E_E(\theta)\sin\phi\hat{e}_\phi - E_H(\theta)\cos\phi\hat{e}_\theta\right], \tag{1b}$$

where $e^{-i\omega t}$ time dependence has been suppressed ($\omega = 2\pi f$, $k = 2\pi/\lambda$), and Z_0 is the impedance of free space. Equations (1)

[1] In principle, one can compute the fields everywhere from the solution to the electric field integral equation (EFIE) for the currents over the surface of the semi-infinite waveguide. And indeed, a numerical EFIE solution leads in Section II-B-2 to approximating the waveguide fringe currents by isotropically radiating line sources. However, we found it impossible to rely entirely on this numerical integral equation solution because it demanded a prohibitive amount of computer time and storage to achieve less than desired accuracy [5].

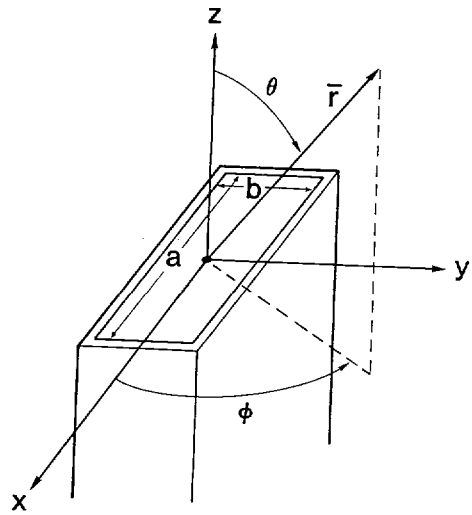

Fig. 1. Geometry of open-ended rectangular waveguide.

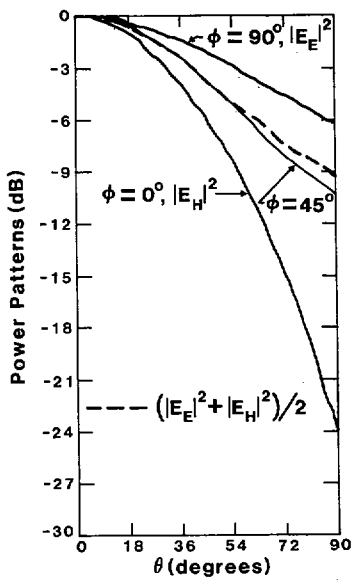

Fig. 2. Measured E_E and E_H power patterns of open-ended rectangular X-band waveguide at 9.32 GHz, and comparison of measured $\phi = 45°$ power pattern with $1/2(|E_E|^2 + |E_H|^2)$ predicted by (1).

immediately reduce the problem of finding the far fields to that of finding the E-plane and H-plane patterns, $E_E(\theta)$ and $E_H(\theta)$, respectively. Indication that (1) represent the far fields of the open-ended waveguide to a rather good approximation in the forward hemisphere can be seen from Fig. 2 which plots the measured power patterns of an X-band waveguide at 9.32 GHz for $\phi = 0°$, 45°, and 90°, and compares the 45° pattern with $\frac{1}{2}[|E_E|^2 + |E_H|^2]$, i.e., with the power pattern predicted by (1) from the measured E- and H-plane patterns. In particular, the ϕ-dependence of (1) conforms more closely to the measured power patterns than the "separable dependence" obtained from aperture integration [2] or the edge diffraction solution [3]. Still, the approximation (1) would not be expected to give very accurate polarization ratios for wide θ angles near $\phi = 45°$.

A. The E-Plane Pattern

The E-plane pattern, $E_E(\theta)$, is predicted quite accurately by inserting the E- and H-fields of the propagating TE_{10} mode into the Stratton-Chu formulas [1, sec. 8.14] and integrating over the open end of the waveguide [2]. Risser states in [2], and we prove in [5], that this Stratton-Chu integration of the TE_{10} fields is equivalent to integrating over the truncated interior surface currents of the propagating TE_{10} mode (incident plus reflected). In other words, the resulting far fields obtained from the Stratton-Chu formulas neglect only the evanescent mode currents inside the waveguide and the surface currents on the outside of the waveguide.

Although these fringe currents[2] can contribute appreciably to the absolute value of the field, they have a minor secondary effect on the broad E-plane pattern which remains well above −10 dB for all angles θ. Thus for $E_E(\theta)$ we simply use the classical result of the aperture integration with the Stratton-Chu formulas [2]

$$E_E(\theta) = A_E \frac{\left[1 + \frac{\beta}{k}\cos\theta + \Gamma\left(1 - \frac{\beta}{k}\cos\theta\right)\right]}{\left[1 + \frac{\beta}{k} + \Gamma\left(1 - \frac{\beta}{k}\right)\right]} \frac{\sin\left(\frac{kb}{2}\sin\theta\right)}{\frac{kb}{2}\sin\theta}. \tag{2}$$

The normalized propagation constant β/k for the TE_{10} mode equals $\sqrt{1 - (\pi/ka)^2}$ and the reflection coefficient of the TE_{10} mode from the end of the waveguide is denoted by Γ. The constant A_E, which remains arbitrary at this point in the derivation, is eventually related to the amplitude of the incident TE_{10} mode through (9) or (14). The factor $[1 + \beta/k + \Gamma(1 - \beta/k)]$ in the denominator of (2) is included merely to simplify the normalization at $\theta = 0$.

Since (2) could be obtained by integrating the truncated TE_{10} surface current, it remains a valid approximation for θ in the back as well as forward hemisphere. Comparisons with measured data show that (2) becomes a slightly better approximation in the forward hemisphere when Γ is set equal to zero. Thus, for the sake of simplicity, convenience, and slightly greater pattern accuracy, Γ can be set equal to zero whenever (2) is used in the forward hemisphere, the region of interest for near-field measurements. Beyond several degrees into the back hemisphere, a more accurate E-plane pattern results by including the reflection coefficient.

In Fig. 3 the amplitude and phase of $E_E(\theta)$ in the forward hemisphere is plotted from (2) and compared with National Bureau of Standards (NBS) measured data for X-band waveguide at 9.32 GHz and for L-band (WR-650) waveguide at 1.0 GHz. The close agreement between the theoretical and experimental curves was somewhat unexpected for the L-band guide because the 1 GHz frequency is approaching the 0.908 GHz cut-off frequency and lies well below the lowest recommended usable frequency of 1.12 GHz.

B. The H-Plane Pattern

The H-plane pattern, $E_H(\theta)$, is much narrower than the E-plane pattern and, consequently, it is more strongly influenced by the fringe currents neglected in the Stratton-Chu integration. Specifically, the Stratton-Chu integration with the TE_{10} mode yields an

[2] Unless otherwise stated, the term "fringe current" refers herein to the actual current at the waveguide edges in excess of the truncated TE_{10} mode current, and not to the fringe current of the corresponding half-plane or parallel-plate waveguide.

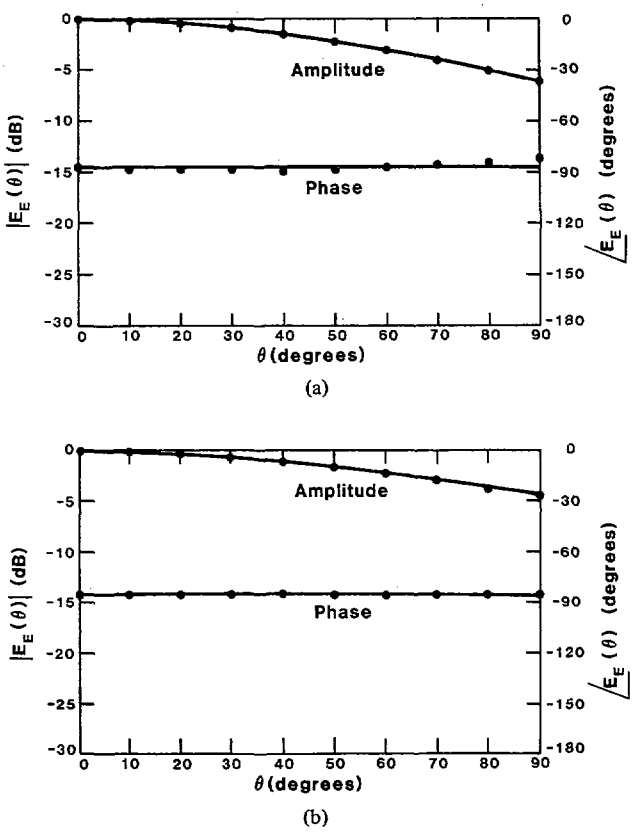

Fig. 3. Amplitude and phase of E-plane field calculated from (2) (——), and measured at NBS (· · ·). (a) X-band rectangular waveguide at 9.32 GHz. (b) L-band rectangular waveguide at 1.0 GHz.

H-plane pattern much broader than the measured pattern whether or not the reflection coefficient Γ is included.

Two separate methods will be developed for determining the H-plane pattern more accurately. This first method, referred to herein as the E-field integration method, does not require the reflection coefficient Γ, but produces an inaccurate H-plane pattern over much of the back hemisphere. The second method, referred to herein as the fringe current method, does require the reflection coefficient but yields an accurate H-pattern for all θ—front and back hemisphere.

1) The E-Field Integration Method for the H-Plane Fields: The Stratton-Chu formulas are not the only expressions that can be used to predict the far fields from an aperture integration of the fields of the TE_{10} mode. In particular, the electric or magnetic field in the forward hemisphere can be expressed, respectively, as a double Fourier transform of the electric or magnetic field alone over the infinite plane just in front of the mouth of the waveguide. Concentrating on the electric field, for reasons that become apparent in the next paragraph, we express the H-plane far field as [6].

$$\bar{E}(r\to\infty,\theta,\phi=0)_{0\leqslant\theta\leqslant\pi/2} = \frac{e^{ikr}}{kr}\frac{k^2}{2\pi}\hat{e}_r\times\hat{e}_z\times\int_{-\infty}^{\infty}\int_{-\infty}^{\infty}\bar{E}(\bar{R}')e^{-ikx'\sin\theta}\,dx'\,dy', \quad (3)$$

where $\bar{R}' = x'\hat{e}_x + y'\hat{e}_y$ is the integration vector from the origin to an area element $dx'dy'$ in the plane of integration.

Now the electric and magnetic field ($\bar{E}_{10}$ and $\bar{H}_{10}$) of the TE_{10} mode is given by

$$\bar{E}_{10} = E_0(1+\Gamma)\cos\left(\frac{\pi x}{a}\right)\hat{e}_y \quad (4a)$$

$$\bar{H}_{10} = -\frac{E_0}{Z_0}\left[(1-\Gamma)\frac{\beta}{k}\cos\left(\frac{\pi x}{a}\right)\hat{e}_x + \frac{\pi}{ika}(1+\Gamma)\sin\left(\frac{\pi x}{a}\right)\hat{e}_z\right], \quad (4b)$$

where E_0 is the arbitrary amplitude of the incident TE_{10} mode. Note that the E-field has but one component and it goes to zero at the edges $x = \pm a/2$. This suggests there will be little difference between the average x-variation of the electric field just in front of the mouth of the waveguide and that of the TE_{10} mode. In other words, for the purpose of determining a reasonably accurate H-plane pattern, the E-field on the integration plane in (3) can be approximated by the $\bar{E}_{10}$ of (4a) over the mouth of the waveguide and zero outside [7]. Performing this simple integration of (3), we find an approximate H-plane pattern given by

$$E_H(\theta)_{0\leqslant\theta\leqslant\frac{\pi}{2}} = A_E\left(\frac{\pi}{2}\right)^2\cos\theta\,\frac{\cos\left(\frac{ka}{2}\sin\theta\right)}{\left[\left(\frac{\pi}{2}\right)^2-\left(\frac{ka}{2}\sin\theta\right)^2\right]}. \quad (5)$$

The constant A_E in (5) is the same as in (2) because $E_E(\theta)$ must equal $E_H(\theta)$ along the boresight direction $\theta = 0$.

The same integration with $\bar{E}_{10}$ does not and would not be expected to yield an accurate E-plane pattern because the average y-variation of the tangential electric field over the infinite aperture plane of integration differs significantly from that of the incident $\bar{E}_{10}$ mode field.[3] Also, substitution of $\bar{H}_{10}$ from (4b) into the magnetic field formula corresponding to (3) produces a very poor approximation for both E- and H-plane far fields. This, of course, is not surprising because the $\bar{H}_{10}$ field does not go to zero at any of the waveguide edges.

Fig. 4 compares the amplitude and phase curves for the H-plane fields in the forward hemisphere calculated from (5), measured at NBS, and calculated from the Stratton-Chu expression for the H-plane pattern given by [2]

$$E_H(\theta) = A_H\,\frac{\left[\left(\cos\theta+\frac{\beta}{k}\right)+\Gamma\left(\cos\theta-\frac{\beta}{k}\right)\right]}{\left[\left(\frac{\pi}{2}\right)^2-\left(\frac{ka}{2}\sin\theta\right)^2\right]}\cdot\cos\left(\frac{ka}{2}\sin\theta\right), \quad (6)$$

with $A_H = -ik^2abE_0/8$.

The H-plane fields predicted by (5) agree well with the measured data even near the L-band cut-off frequency, and they are considerably closer (on a linear scale) to the measured values than those predicted by the result (6) of the Stratton-Chu formulas.

[3] For rectangular waveguide with an infinite flange on which the tangential electric field is held zero, this E-field integration of $\bar{E}_{10}$ predicts a far-field pattern over the entire hemisphere that is very close to the exact field [16].

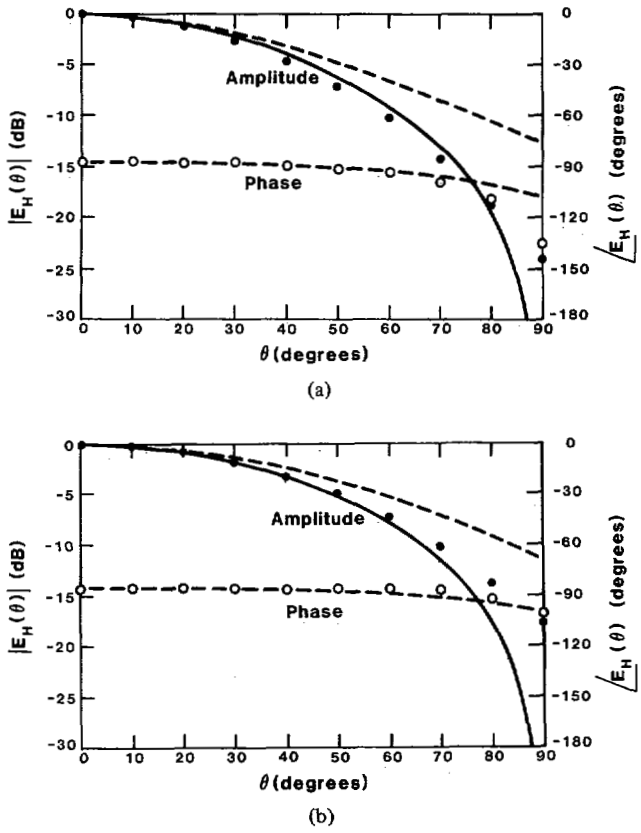

Fig. 4. Amplitude and phase of H-plane field calculated from (5) (——), calculated from Stratton-Chu formulas (---), and measured at NBS (···). The H-plane phase from (5) is not shown because it is simply a constant phase of about $-90°$ found from (9). (a) X-band rectangular waveguide at 9.32 GHz. (b) L-band rectangular waveguide at 1.0 GHz.

2) The Fringe Current Method for the H-Plane Fields: Although the integrated E-field expression (5) for the H-plane pattern is more accurate in the forward hemisphere than the previous expressions [2], [3], it has a couple of shortcomings that the E-plane expression (2) does not have. First, the expression (5) does not remain accurate in the back hemisphere because it was derived from (3) which applies only to the front, free-space hemisphere. Thus, when the constant A_E is related to total power radiated, the H-plane pattern in the back hemisphere must be roughly estimated and this estimation introduces an additional, albeit small, inaccuracy into the determination of gain (see Section III). Secondly, the expression (5) approaches zero like $\cos\theta$ as θ approaches 90°, and predicts too low an H-plane pattern for θ between about 70° and 90°. Fortunately for all near-field antenna measurements, except those made with the probe extremely close to the test antenna, the pattern of the probe beyond 70° does not intercept the test antenna and thus does not affect the probe correction [8]-[12]. However, for the sake of those rare exceptions as well as for slightly more reliable estimates of gain, we derive an alternative expression to (5) for the H-plane pattern that remains a good approximation for all values of θ.

To derive this alternative expression, return to a formulation of the open-ended waveguide problem in terms of surface currents. From the symmetry of the rectangular waveguide and TE_{10} mode, only y-directed currents contribute to the H-plane fields. Thus, (6) neglects only the fringe currents along the $x = \pm a/2$ edges of the open end of the waveguide (provided the finite wall thickness of the waveguide is ignored).

We first tried to obtain a good estimate of the y-directed fringe currents by looking at the $x = \pm a/2$ edges as part of the infinite edge of a half-plane. The exciting field was taken as the incident *and reflected* plane wave produced by the incident and reflected TE_{10} mode. Since (6) is an exact closed-form expression for the H-plane contribution from the truncated TE_{10} mode current, the only additional information one needs is the far fields of the fringe currents of the half-plane E-wave problem. For this problem, these fringe currents produce a far field that is also expressible by an exact, closed-form expression derived by Ufimtsev for the general wedge [13]. For the half-plane the Ufimtsev expression reduces to a simple function involving only sines and cosines of the observation angle and the angle of plane-wave incidence [14].

It is shown in [5, appendix II] that this half-plane current correction works very well for the open-ended parallel-plate waveguide excited by the TE_{10} mode, but unfortunately for the open-ended rectangular waveguide, it did not bring the predicted H-plane pattern to within the desired 1 or 2 dB accuracy of the measured pattern at the wider angles of observation. The reason for the greater inaccuracy in the case of the rectangular waveguide is simply that the top and bottom edges of the rectangular waveguide strongly influence the edge diffraction from the $x = \pm a/2$ side edges, and produce fringe currents significantly different from those of the half-plane problem.

We were finally able to obtain a more accurate estimate of the fringe currents on the $x = \pm a/2$ sides of the rectangular waveguide from a numerical solution to the EFIE applied to the open-ended rectangular waveguide [5], [15]. The numerical EFIE solution revealed that to a good approximation the fringe currents at $x = \pm a/2$ of the waveguide, unlike the fringe currents of the half-plane, contributed to the H-plane pattern as line sources that radiate *isotropically* with θ, or specifically as

$$A_H C_0 \cos\left(\frac{ka}{2}\sin\theta\right), \tag{7}$$

where C_0 is a positive real constant. Adding (7) to (6) then determines the H-plane pattern derived by the fringe current method

$$E_H(\theta) = A_H\left[\frac{\left(\cos\theta + \frac{\beta}{k}\right) + \Gamma\left(\cos\theta - \frac{\beta}{k}\right)}{\left(\frac{\pi}{2}\right)^2 - \left(\frac{ka}{2}\sin\theta\right)^2} + C_0\right] \cdot \cos\left(\frac{ka}{2}\sin\theta\right). \tag{8}$$

The constant A_H is defined under (6) and the E-plane constant A_E in (2) is related to A_H by $E_E(0) = E_H(0)$, or

$$A_E = A_H\left\{\left(\frac{2}{\pi}\right)^2\left[\left(1 + \frac{\beta}{k}\right) + \Gamma\left(1 - \frac{\beta}{k}\right)\right] + C_0\right\}. \tag{9}$$

The positive real constant C_0, which depends on the frequency and the waveguide dimensions, remains the one unknown in the fringe current expressions (8) and (9). A simple way to find C_0 is to equate the radiated power P_r determined from the far field (1) (with (2) and (8) inserted) to the total input power P_0 determined from the TE_{10} mode fields (4), and to solve the result-

ing quadratic equation for C_0. From (1) and (4), P_0 and P_r are found to be, respectively,

$$P_0 = \frac{ab|E_0|^2(1-|\Gamma|^2)\beta/k}{4Z_0} \tag{10a}$$

$$P_r = \frac{\pi}{2Z_0k^2}\int_0^{\pi}(|E_E(\theta)|^2 + |E_H(\theta)|^2)\sin\theta d\theta. \tag{10b}$$

Assuming the resistive loss in the waveguide walls is negligible, we equate (10a) and (10b) to find

$$a_qC_0^2 + 2b_qC_0 + c_q = 0 \tag{11a}$$

or

$$C_0 = \frac{-b_q + \sqrt{(b_q)^2 - c_qa_q}}{a_q}, \tag{11b}$$

where a_q, b_q, and c_q are constants determined by the integrals in (10b) of the E- and H-plane patterns, (2) and (8).

The complex reflection coefficients over the recommended usable bandwidth of the X-, C-, and L-band waveguides, needed to determine C_0 from (11b), were obtained from measurements with an automatic network analyzer at NBS. The amplitude and phase of these measured Γ are shown in Fig. 5.[4]

Using these measured reflection coefficients and the C_0 evaluated from (11b), the amplitude and phase of the H-plane pattern (8) is plotted in Fig. 6 for the forward hemisphere of X-band waveguide at 9.32 GHz and L-band waveguide at 1.0 GHz. These predicted H-plane patterns (8) derived from the fringe current method agree well with measured patterns even near $\theta = 90°$ and, though not shown in Fig. 6, over the back hemisphere. The patterns of Fig. 6 display an accuracy representative of (8), i.e., about 2 dB or better accuracy 90° off boresight with rapidly increasing accuracy toward boresight.

The disadvantages of using (8) instead of the expression (5), which was derived from the E-field method, are the extra computations needed to evaluate C_0 and the requirement of the reflection coefficient Γ. To determine C_0 from (11b), the far-field integrals in (10b) were computed with the reflection coefficient in the E-plane (2) used only beyond several (fifteen) degrees into the back hemisphere, in accordance with the recommendation of Section II-A for slightly more accurate E-plane fields.

III. DETERMINATION OF ON-AXIS GAIN

Two approximations have been derived for the far fields of open-ended rectangular waveguides. The first uses (2) and (5), and the second uses (2) and (8) for the E- and H-plane patterns in (1). This section evaluates the absolute on-axis gain predicted by each approximation.

Because the resistive loss in the walls of the waveguide is negligible, the total radiated power P_r must equal the net input power P_0, and the on-axis gain G_0 becomes equal to the on-axis directivity:

$$G_0 = \frac{4\pi r^2|\bar{E}(r\to\infty,\theta=0)|^2}{2Z_0P}, \quad P = P_0 = P_r. \tag{12}$$

[4] The L-band reflection coefficient was estimated by scaling the given Ku-band data, since b/u for L- and Ku-band waveguide are the same and L-band data was not immediately available. Of course, some error is introduced by this scaling because the wall thickness of Ku- and L-band waveguides do not scale like the inner dimensions.

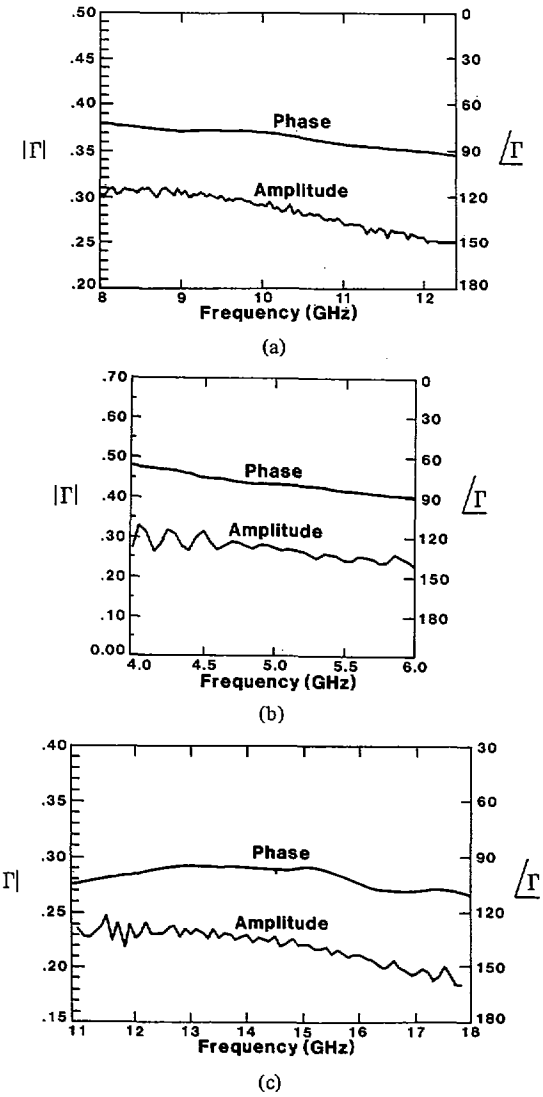

Fig. 5. Measured amplitude and phase (with respect to end) of reflection coefficients for X-, C-, and Ku-band open-ended standard rectangular waveguide. (a) X-band. (b) C-band. (c) Ku-band.

The gain G_{01} predicted by (2) and (5) is found from (12) by using (10b) for the total power radiated, (2) with $\Gamma = 0$ for the E-plane pattern, and (5) for the H-plane pattern;

$$G_{01} = 4\Big/\int_0^{\pi}\left\{\left[\frac{\left(1+\frac{\beta}{k}\cos\theta\right)\sin\left(\frac{kb}{2}\sin\theta\right)}{\left(1+\frac{\beta}{k}\right)\frac{kb}{2}\sin\theta}\right]^2 + \left[\left(\frac{\pi}{2}\right)^2\frac{\cos\theta\cos\left(\frac{ka}{2}\sin\theta\right)}{\left(\frac{\pi}{2}\right)^2-\left(\frac{ka}{2}\sin\theta\right)^2}\right]^2\right\}\cdot\sin\theta d\theta. \tag{13}$$

Note that the arbitrary constant A_E for the approximate formulas (2) and (5) cancels in the determination of gain from (13). If desired, the magnitude of A_E for (2) and (5) can be written in terms

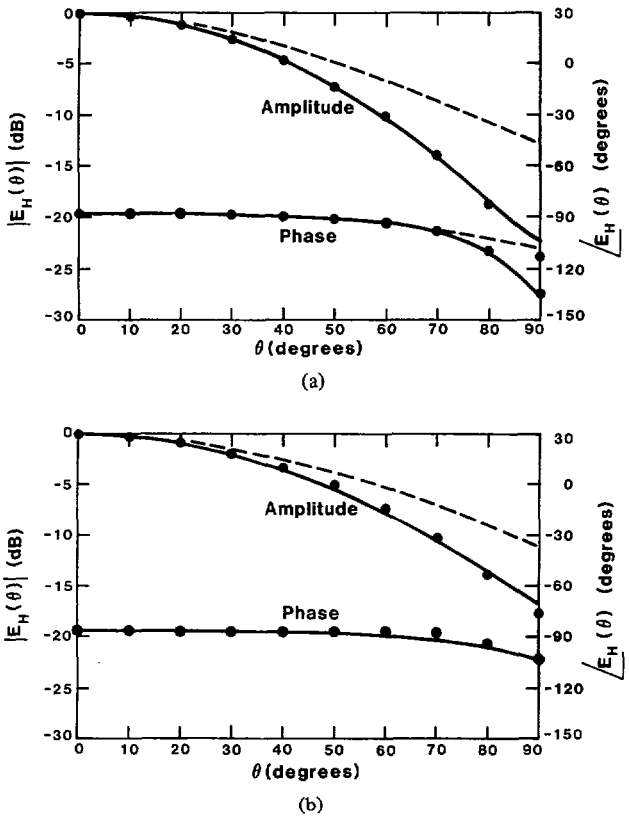

Fig. 6. Amplitude and phase of H-plane field calculated from (8) (——), calculated from Stratton–Chu formulas (---), and measured at NBS (· · ·). (a) X-band rectangular waveguide at 9.32 GHz. (b) L-band rectangular waveguide at 1.0 GHz.

of the coefficient E_0 of the incident TE_{10} mode by simply equating P_0 and P_r to get

$$|A_E|^2 = \frac{k^2 ab(1-|\Gamma|^2)\dfrac{\beta}{k}}{2\pi\,(\text{denom})}|E_0|^2, \tag{14}$$

where "denom" denotes the integral denominator of the right side of (13).

Since we want to avoid using the reflection coefficient in determining gain from (13), both the E- and H-plane patterns in the integral denominator of (13) are simply chosen constant beyond 15° into the back hemisphere. Although this particular choice for the back hemisphere is not critical to the evaluation of gain because the power radiated into the back hemisphere is a small fraction of the total power radiated, some reasonable choice for the back-hemisphere pattern must be made to evaluate the gain accurately from (13).

The gain G_{02} predicted by the approximate formulas (2) and (8) is found in terms of the constant C_0 (which is computed from (11b) through the definition of gain (12) with $P = P_0$ substituted from (10a), and the on-axis far field inserted from (2) or (8);

$$G_{02} = \frac{\pi k^2 ab}{8\dfrac{\beta}{k}(1-|\Gamma|)^2}\left|\left[1+\frac{\beta}{k}+\Gamma\left(1-\frac{\beta}{k}\right)\right]\left(\frac{2}{\pi}\right)^2 + C_0\right|^2. \tag{15}$$

Gain curves computed from (15) as well as (13) are drawn in

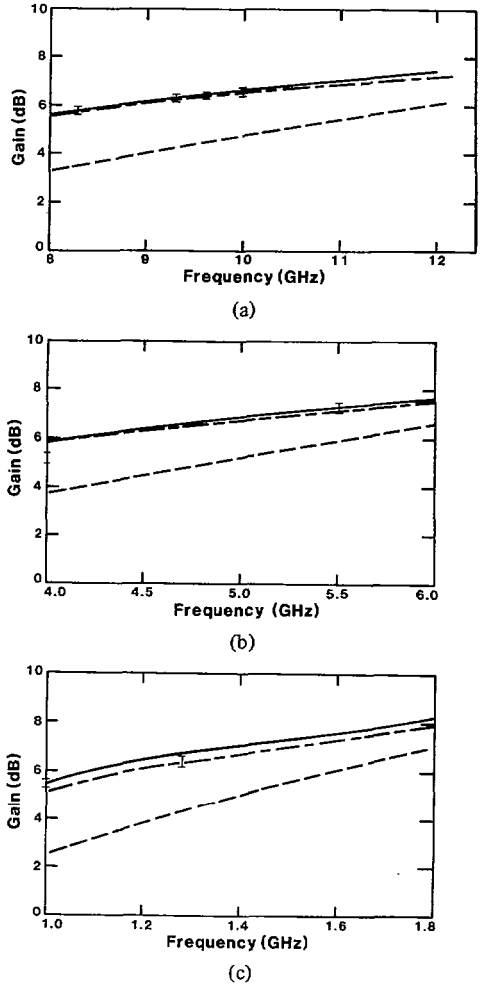

Fig. 7. On-axis gain of open-ended rectangular waveguide calculated from (13) (——), (15) (——), and the Stratton–Chu formulas (---). The I symbols denote NBS measured values of gain and estimated limits of error. (a) X-band, (b) C-band. (c) L-band.

Fig. 7, which shows the considerable improvement in gain values of both (15) and (13) over the gain determined from the classical Stratton-Chu results [2].[5] The comparison of measured and predicted values of gain in the Fig. 7 indicates that the formulas (15) and (13) predict gain with an accuracy of about 0.2 dB. The "two-sigma" limits of error shown in Fig. 7 by the "I" symbols for the measured data were obtained from internal NBS reports of near-field antenna measurements.

IV. CONCLUSION

This work was motivated by the need for simple, accurate expressions for the far field and gain of open-ended rectangular waveguide probes used in making near-field antenna measurements. Except near the E-plane, previous expressions based on either the Stratton-Chu formulas or an edge diffraction solution predict patterns that deviate from measured patterns to the extent that their predicted gain values are 2 to 3 dB too low. The alternative expressions for the far fields developed here reduce this inaccuracy by about a factor of ten throughout the recommended usable bandwidth of X-band and larger standard rectangular wave-

[5] The computations of gain from the Stratton–Chu expressions used measured values of reflection coefficient. The Stratton–Chu gain curves fall further below the measured gain if the reflection coefficient is assumed zero.

guide. For *Ku*-band and smaller standard waveguide, the wall thickness becomes an appreciable fraction of the waveguide cross-sectional dimensions and the approximate formulas may become less accurate.

Two alternative sets of approximate formulas were derived for the far fields–(2) and (5), or (2) and (8), inserted into (1). The former set, (2) and (5), approximates the far fields in the forward hemisphere without requiring the TE_{10} reflection coefficient for the open-ended waveguide, but predicts too narrow an *H*-plane pattern for angles near 90° off boresight. The latter set, (2) and (8), requires the reflection coefficient, but yields a reliable estimate of the radiation pattern in all directions, including the back hemisphere.

Both sets of formulas assume first-order azimuthal dependence. Although this approximation provides more accurate power patterns than those obtained from the separable approximations of previous formulas, none of the formulas predict accurate polarization ratios far away from boresight near the 45° planes. Another shortcoming of all the formulations is their failure to predict the reflection coefficient of the TE_{10} mode from the end of the waveguide.[6] Thus the statement Risser [2, p. 336] made 35 years ago still applies: "A more rigorous treatment of the problem would be desirable."

ACKNOWLEDGMENT

Allen C. Newell, David A. Hill, Ronald C. Wittmann, and Richard L. Lewis of the National Bureau of Standards, and Professor Jung-Woong Ra of the Korea Advanced Institute of Science and Technology contributed generously to this work through their helpful discussions and reviews. Allen C. Newell, Douglas P. Kremer, Stanley B. Kilgore, and Bill C. Yates of NBS performed and supplied the far-field, gain, and reflection coefficient measurements of the open-ended rectangular waveguide probes.

REFERENCES

[1] J. A. Stratton, *Electromagnetic Theory*. NY: McGraw-Hill, 1941.

[2] J. R. Risser, "Waveguide and horn feeds," ch. 10 in *Microwave Antenna Theory and Design*, S. Silver, Ed. NY: McGraw-Hill, 1949.

[3] C. E. Ryan, Jr. and R. C. Rudduck, "Radiation patterns of rectangular waveguides," *IEEE Trans. Antennas Propagat.*, vol. AP-16, pp. 488–489, July 1968.

[4] E. Comforti and A. J. Giarola, "Outside surface experimental currents in open-ended circular waveguide," *Inst. Elec. Conference Publication 219 of the Third International Conference on Antennas and Propagation*, Univ. East Anglia, U.K., pt. 1, pp. 123–126, Apr. 1983.

[5] A. D. Yaghjian, "Approximate formulas for the far fields and gain of open-ended rectangular waveguide," *Nat. Bur. Stand. Internal Rep.*, 83-1689, May 1983.

[6] C. C. Johnson, *Field and Wave Electrodynamics*. NY: McGraw-Hill, 1965, eq. 10.26.

[7] J. J. Epis, "Compensated electromagnetic horns," *Microwave J.*, vol. 4, pp. 84–89, May 1961.

[8] A. D. Yaghjian, "Upper-bound errors in far-field antenna parameters determined from planar near-field measurements, Part I: Analysis," Nat. Bur. Stand. Tech. Note 667; sec. II.A.3, Oct. 1975.

[9] ——, "Efficient computation of antenna coupling and fields within the near-field region," *IEEE Trans. Antennas and Propagat.*, vol. AP-30, pp. 113–128, Jan. 1982.

[10] ——, "Near-field antenna measurements o a cylindrical surface: A source scattering-matrix formulation," Nat. Bur. Stand. Tech. Note 696, sec. 4.2.1, Sept. 1977.

[11] D. M. Kerns, "General formula for voltage induced in a receiving antenna," in *Digest Nat. Radio Sci. Meeting*, Boulder, CO, Nov. 1978, p. 14.

[12] D. W. Hess, "Practical considerations for near-field measurements and the use of probe correction," in *Dig. Nat. Radio Sci. Meeting*, Boulder, CO, Jan. 1982, p. 186.

[13] P. Ia Ufimtsev, "Approximate computation of the diffraction of plane electromagnetic waves by certain bodies, Part I and II," *Sov. Phys.-Tech. Phys.*, vol. 2, pp. 1708–1718, Aug. 1957; vol. 3, pp. 2386–2396, Nov. 1958.

[14] K. M. Mitzner, "Incremental length diffraction coefficient," Air Force Avionics Lab. Tech. Rep. 73-296, sec. 2.2.5, Apr. 1974.

[15] A. W. Glisson, and D. R. Wilton, "Simple and efficient numerical methods for problems of electromagnetic radiation and scattering from surfaces," *IEEE Trans. Antennas and Propagat.*, vol. AP-28, pp. 593–603, Sept. 1980.

[16] R. H. MacPhie and A. I. Zaghloul, "Radiation from a rectangular waveguide with infinite flange—exact solution by the correlation matrix method," *IEEE Trans. Antennas Propagat.*, vol. AP-28, pp. 497–503, July 1980.

[17] B. N. Das, "Admittance of rectangular apertures," *J. Inst. Electron. Telecommun. Eng.*, India, vol. 22, pp. 133–137, Mar. 1976.

[6] A rough estimate of the reflection coefficient can be made in terms of the complex power in the plane-wave spectrum associated with the approximate far fields [17].

Arthur D. Yaghjian (S'68–M'69), for a photograph and biography please see page 128 of the January 1982 issue of this TRANSACTIONS.